bladder filling affects DIR performances only in the case where no controlling ROI is selected or when only the bladder is exploited as controlling ROI. The statistical test shows significant differences on the DSC results between the DIR obtained selecting as controlling ROIs all the available ROIs and the DIR obtained without controlling ROIs or only when a subset of controlling ROIs is selected (bladder or bladder, prostate and rectum). As far as the CC concern, significant differences were observed only between DIR computed exploiting as controlling ROIs all the delineated ROIs and DIR performed without the selection of controlling ROIs or, for the real patient CT case only, where the bladder was selected as controlling ROI.

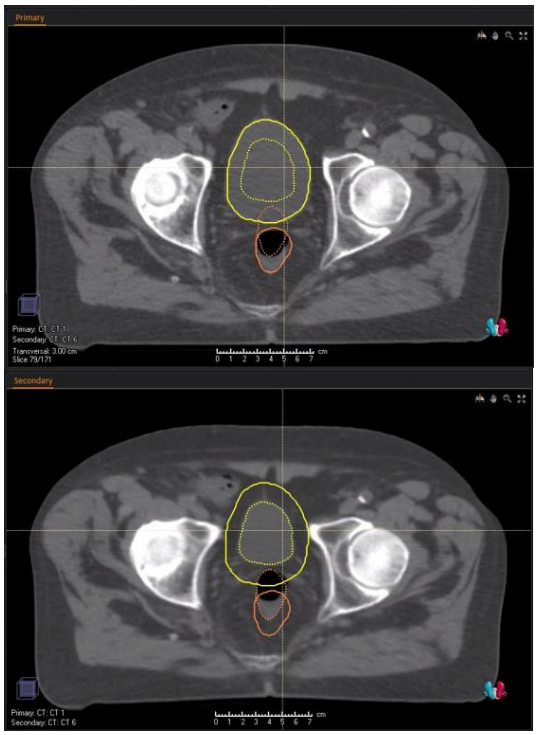

Conclusion

ANACONDA performances improve increasing the number of selected controlling ROIs approaching a saturation level after the selection of a defined ROIs subset. This would suggest to reduce the number of controlling ROIs delineated in clinical practice thus decreasing the time spent to contour each patient CT.

EP-2067 Data driven region of interest respiratory surrogate signal extraction from CBCT data

A. Akintonde[1,2], H. Grimes[3], S. Moinuddin[3], R.A. Sharma[4], J. McClelland[1], K. Thielemans[2]

[1]University College London, Centre for Medical Image Computing- Department of Medical Physics and Biomedical Engineering, London, United Kingdom ; [2]University College London, Institute of Nuclear Medicine, London, United Kingdom ; [3]University College London Hospital, Department of Radiotherapy Physics, London, United Kingdom ; [4]University College London, Cancer Institute, London, United Kingdom

Purpose or Objective

Cone-beam CT (CBCT) scans performed during a course of radiotherapy can be degraded by respiratory motion. 4D reconstruction or motion-compensated (MC) reconstruction can be used to visualise or compensate for the motion. Both techniques require a respiratory surrogate signal. Surrogate signals derived directly from the projection data are appealing as they require no extra equipment and may have a stronger relationship to the internal motion than signals from external devices. In this study, we developed a novel method for extracting a surrogate signal directly from CBCT data, and we compared it to the Amsterdam Shroud technique.

Material and Methods

A region of interest (ROI) corresponding to either the tumour or diaphragm was selected, and the ROI in the projection data was enhanced by digitally removing the rest of the anatomy. PCA was applied to groups of adjacent projections using a sliding-window approach, and a novel technique used to combine the extracted signals from each window to generate a coherent respiratory signal from the entire data set.

We evaluated our method using four simulated CBCT acquisitions (three standard, one extended) that emulate clinical conditions and were generated with the XCAT computer phantom and real patient respiratory traces as the ground truth (GT) signals. Simulations were performed using OpenRTK. We assessed the signals extracted from the tumour ROI (T-ROI) and the diaphragm ROI (D-ROI) by calculating the correlation coefficient (CC) with the GT signal. For comparison, we extracted a signal generated using a modified Amsterdam Shroud (M-AS) technique, which corrects for the drift that can be present in the original Amsterdam Shroud signal. Finally, phase sorted 4DCBCT images were reconstructed for the extended acquisition using the GT, T-ROI, and M-AS signals.

Results

Figure 1 shows the different signals for the four simulated acquisitions, also shown are the corresponding CC obtained for each simulation. Figure 2 shows the 4DCBCT reconstructions generated using the different signals. It can be seen that the 4DCBCT images from the T-ROI signal closely resemble the images from the GT signal, whereas the images from the AS signal show clear motion artefacts.

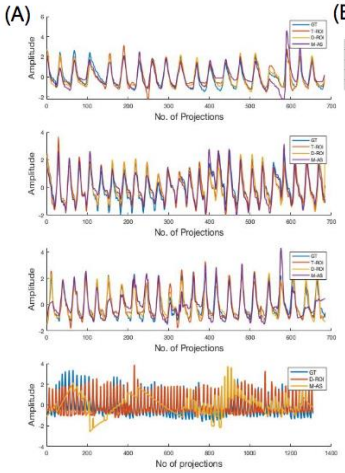

	T-ROI	D-ROI	M-AS
Simulation 1	0.91	0.94	0.84
Simulation 2	0.91	0.90	0.90
Simulation 3	0.94	0.95	0.83
Simulation 4	0.87		0.02

Figure 1.0. (A) Respiratory signals obtained from 4 different simulations. The first 3 simulations were standard acquisition with the tumour and diaphragm region in the FOV of the projections, where the last simulation corresponds to an extended acquisition where the diaphragm was not in the FOV. Plots show the signals obtained using our method from 2 ROIs (D-ROI and T-ROI), the M-AS method and the GT. For the last simulation, D-ROI is not shown as not available. **(B)** Correlation coefficients between the extracted signals, M-AS, and the ground truth signals for the different simulations

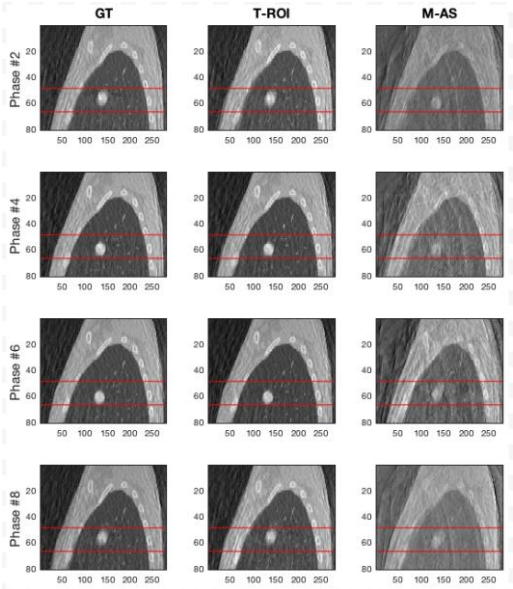

Figure 2.0. Sagittal planes of the images reconstructed from respiratory sorted phase bins using the GT motion, our proposed method and the M-AS technique respectively. Each row corresponds to a particular phase bin, shown here are the 2nd , 4th ,6th and 8th bins (out of 8) respectively. These phases were chosen to highlight the extent of the tumour motion. The red horizontal lines are positioned to show the extent of the tumour motion.

Conclusion

We have developed a novel method of extracting respiratory motion from CBCT projection data. The method allows selecting a ROI to target the respiratory motion of interest. We evaluated our method on XCAT simulations and compared it to the well-known Amsterdam Shroud technique, combined with a simple method for baseline-drift correction. High correlations were obtained between signals from our proposed method and the ground truth for all simulations, achieving better correlations than when using AS. The preliminary evaluation shows that the proposed technique is therefore a potential candidate for a robust basis for respiratory motion management without need for external equipment. In future, we plan to apply this method to patient data.

EP-2068 Scatter-corrected CBCTs for online water-equivalent path length calculations in proton therapy

A.G. Andersen[1], U.V. Elstrøm[2], B. Winey[3], J.B.B. Petersen[2], M. Falk[1], P. Skyt[1], O. Nørrevang[1], C. Grau[4], L.P. Muren[1]

[1]Danish Centre for Particle Therapy, Department of Medical Physics, Aarhus, Denmark ; [2]Aarhus University Hospital, Department of Medical Physics, Aarhus, Denmark ; [3]Massachusetts General Hospital, Department of Medical Physics, Boston- MA, USA ; [4]Aarhus University Hospital, Department of Oncology, Aarhus, Denmark

Purpose or Objective

Releasing the full potential of proton therapy requires mitigation of proton range variations caused by density/anatomy changes during the course of treatment. Cone-beam CT (CBCT) scanners are becoming available at proton gantries, but scatter and other artefacts deteriorate the accuracy of the Hounsfield unit representation in the CBCTs, with implications for online proton range or dose calculations. *A priori* scatter correction algorithms have shown promising results for reducing CBCT artefacts. Proton range calculations based on scatter corrected CBCTs have not yet been compared directly to calculations on conventional CTs in patients. The aim of this study was therefore to do such a comparison using mid-course CTs of head and neck cancer patients.

Material and Methods

Our scatter correction algorithm initially used rigid and deformable registration of the planning CT (pCT) to a raw reconstruction of the CB projections (rawCBCT). The deformed CT was then forward projected onto the same geometry as that of the CB projections, from which the forward projections were subtracted. The differential projections were then smoothed with a low-pass gaussian filter, to create a scatter map which was then subtracted from the original CB projection before a final reconstruction (corrCBCT). For comparison we also used our clinical reconstruction of the CB projection (clinCBCT), which used the adaptive scatter kernel superposition method (Varian iTools). The pCT, a mid-course CT (mCT) and CB projections acquired the same day as the mCT from four head and neck patients previously treated with photon-based radiotherapy were analysed. Proton ranges, i.e. water-equivalent path lengths (WEPLs), were calculated in planar projections of all voxels in the patients, using the pCT as reference. WEPL maps for the mCT were subtracted from both the corrCBCTs and the clinCBCTs, under the assumption that the patient anatomy changes between the mCT and the CBCT were negligible.

Results

In three of the four patients, the WEPL maps based on the corrCBCT deviated less from the WEPL maps based on the mCT compared to the clinCBCT (Fig 1). In one case the average across the subtracted WEPL map was reduced from 7 mm to 2 mm, with the fraction of the WEPL maps with deviations exceeding +/- 10 mm reduced from 41% with clinCBCT to 19% using the corrCBCT. In the fourth case the averages were within 0.5 mm.

Conclusion

Scatter correction of CBCTs translates into clinically relevant improvements in CBCT-based WEPL calculations, opening a potential for online proton range verification/monitoring.

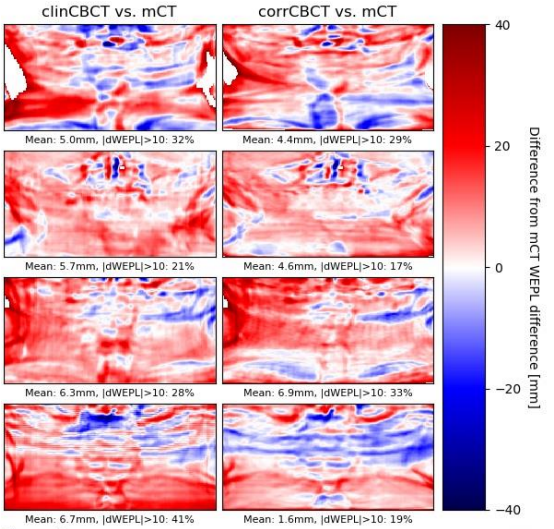

Figure 1:

The difference between the WEPL difference of the pCT and mCT, and the WEPL difference of the pCT and the two CBCT reconstructions, in units of mm WEPL. The corrCBCT reconstruction to the right and the clinCBCT to the left. Each row corresponds to one patient.

EP-2069 Improved dose calculation on CBCT using polyenergetic quantitative (Polyquant) reconstruction

J. Mason[1], W. Nailon[2], A. Perelli[1], S. Andiappa[2], M. Davies[1]

[1]The University of Edinburgh, School of Engineering, Edinburgh, United Kingdom ; [2]Edinburgh Cancer Centre-